Process optimization for production of sub-20 nm soft x-ray zone plates

S. J. Spector[a] and C. J. Jacobsen
Department of Physics, SUNY at Stony Brook, Stony Brook, New York 11794

D. M. Tennant
Lucent Technologies, Bell Laboratories, Holmdel, New Jersey 07733

(Received 28 May 1997; accepted 28 July 1997)

We report here the optimization of processes for producing sub-20 nm soft x-ray zone plates, using a general purpose electron beam lithography system and commercial resist technologies. We have critically evaluated the failure point of the various process steps and where possible chosen alternate methods, materials, or otherwise modified the process. Advances have been made in most steps of the process, including the imaging resist, pattern conversion for electron beam exposure, and pattern transfer. Two phase shifting absorber materials, germanium and nickel, were compared. Zone plates with 30 nm outer zones have been fabricated in both germanium and nickel with excellent quality using polymethyl methyl accrylate and zones as small as 20 nm have been fabricated in nickel using the calixarene resist. The total efficiency as well as the efficiency of different regions of the zone plates were measured. All zone plates have demonstrated good efficiencies, with nickel zone plates performing better than germanium zone plates.
[S0734-211X(97)02306-8]

I. INTRODUCTION

X-ray microscopy provides a unique method for investigation of biological and other samples at high resolution. X-ray microscopy offers the ability to image thick, wet, hydrated samples, and it offers unique contrast mechanisms, such as absorption contrast or x-ray spectroscopic data.[1,2] The spatial resolution of x-ray microscopy is superior to optical microscopy, although not as fine as electron microscopy. The resolution that can be achieved in an x-ray microscope is presently limited by x-ray lens technology.

Fresnel zone plates are the highest resolution optics presently available for soft x rays. The fabrication of Fresnel zone plates offers serious challenges in microfabrication. The transverse image resolution δ_t is approximately equal to the outer zone width δ_{r_N}, so very small, periodic features are necessary. This resolution is achieved only when all zones are correctly positioned to within about a third of their width.[3] Also, the thickness of the zones should be sufficient to adequately attenuate or phase-shift the transmitted x-ray front. This leads to requirements for patterning accuracy of about 1 part in 10^4, and height-to-width aspect ratios as high as possible (6:1 is typical at present).

We describe here the optimization of a process for producing high resolution zone plates. To avoid the expense of a custom *e*-beam lithography system for zone plate fabrication,[4–6] we fabricated Fresnel zone plates using a commercially available electron beam lithography system in a multipurpose microfabrication laboratory. In this standard setup, with no special equipment but with modification of the pattern-generating software, we have fabricated zone plates with outer zone widths as small as $\delta_{r_N}=30$ nm in germanium and as small as $\delta_{r_N}=20$ nm in nickel. The zone plates which have been tested show good efficiency and resolution.

The zone plates were fabricated for and tested on the scanning x-ray transmission microscope (STXM) at the X1A beamline at the National Synchrotron Light Source. In the STXM, a zone plate is illuminated with nearly plane wave illumination. The focal spot of the zone plate forms a microprobe in the sample. The transmitted x rays are detected and an image is formed as the sample is scanned. Because zone plates are diffractive optical elements which are not 100% efficient, it is necessary to have a central stop on the zone plate and to use a pinhole or order sorting aperture to block the unwanted x rays.

II. FABRICATION

The zone plates were fabricated on Si_3N_4 membranes, about 120 nm thick, fabricated following the method of Pawlak *et al.*[7] These membranes are between 38% and 67% transmissive in the wavelength range between 2.4 and 4.5 nm. The membranes were fabricated from Si_3N_4 coated silicon (Si) wafers which are bought commercially.

Before the fabrication of the high resolution nickel or germanium features, gold alignment crosses and thick gold central stops were fabricated. The alignment crosses were fabricated first of 100 nm of gold using lift-off;[8] they are used to align the fabrication of the zones with the central stop. The central stops were then fabricated in 300 or 500 nm of gold in a similar step with a thicker bilayer resist. A large number (>150) central stops or crosses can be fabricated simultaneously for subsequent use in zone plate fabrication.

A. Electron beam exposure and ring conversion software

The zone plates were patterned using the JEOL JBX-6000FS electron beam (*e*-beam) lithography system at Lucent Technologies, Bell Laboratories. The JBX-6000FS sys-

[a]Present address: Lucent Technologies, Bell Labs, Brookhaven National Labs., Bldg. 510E, Upton, NY 11973; Electronic mail: spector@xray1.physics.sunysb.edu

tem has a thermal-field-emission source which operates at 50 keV and can deliver 500 pA current into a 7 nm spot size. For exposure of the 80-μm-diam zone plates, using polymethyl methyl accrylate (PMMA), a beam current of 100 pA was used. The sample stage position is monitored by an interferometer with $\lambda/128 \simeq 5$ nm resolution. The interferometer feeds back to the deflector to correct for any stage position error and is also used as a standard for adjusting the gain and rotation of a writing field.

The JBX-6000FS is a rectangular coordinate system which builds patterns from lines, rectangles, and certain trapezoids with a minimum pixel size of 2.5 nm at the settings we have used. To draw zone plates, one must express rings with given outer and inner radii in terms of these rectangular coordinate primitives. The original software provided by the manufacturer generated rings using an unnecessarily large number of primitives which posed problems not only in file size but especially in unevenness of exposure.[9] An upgraded version of the software is now available from the manufacturer which has been shown by users to provide a 40% reduction in 50 nm zone plate file size and some improvement in exposure quality.[10] We have independently developed our own software for ring generation which results in a tenfold reduction in file size, and which includes two improvements which are crucial to fabrication of the highest resolution zone plates:

(1) radii are calculated using floating point rather than integer math, correcting a ± 2.5 nm error in ring positions at angles other than 0° and 90°; and
(2) we eliminate the double-writing of pixels at the boundaries of primitives.

The algorithm for doing this is described in detail elsewhere,[9] and could potentially be used for other rectangular coordinate machines. The software significantly improved the quality of the exposures, as evidenced by an increase in exposure latitude and a reduction in systematic linewidth variations.

B. Resists

We have found that a thin layer (30–40 nm) of PMMA with a molecular weight of 950 K. Daltons works well for zone plates with outer zones $\geqslant 30$ nm. The PMMA is baked at a temperature of 160 °C overnight. Compared to cooler bake temperatures, we have found that a bake temperature of 160 °C improves the resolution performance of PMMA, while decreasing its sensitivity. This is consistent with increased cross-linking of the PMMA, which may occur at higher bake temperatures.[11] Exposures are done with doses near 500 μC/cm^2. After exposure, the PMMA is developed in 1:2 methyl isobutyl ketone (MIBK): isopropanol (ISO) for 15 s and rinsed in ISO for 45 s.

To achieve higher resolution we have found that PMMA is no longer adequate. To obtain results which can be readily be reproduced we have chosen an alternative resist which is commercially available. A new resist, called calixarene, developed by NEC, provides increased resolution performance.[12] Additionally, the calixarene resist has greater etch resistance making it possible to use a very thin ($\sim$20 nm) layer of resist. The calixarene resist is much slower; our experience has been that it requires $\sim$25 times the dose of PMMA. Using a beam current of 500 pA it is possible to expose an 80-μm-diam zone plate in about 20 min.

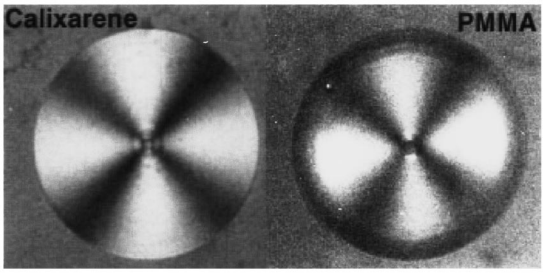

FIG. 1. Differential interference contrast image of 20 nm outer zone width zone plates transferred into 10 nm of germanium. The calixarene resist (left) was successfully patterned, whereas the outer zones in PMMA (right) were not, as evidenced by the cross pattern not extending the entire circle. The cross pattern is a result of the dichroism caused by properly formed zones.

Figure 1 shows a comparison between 20 nm zone plates fabricated in PMMA and calixarene. The process used for calixarene is that described by Fujita *et al.*[12] except a shorter development time of 15 s was used. The pattern was transferred to a 10 nm layer of germanium to make the zones visible. The PMMA zone plate shown is the best of several zone plates fabricated while varying the exposure dose. The figure indicates that the outer zones of the PMMA zone plate were not successfully patterned, but the outer zones of the calixarene zone plate might be. Figure 2 shows the successful transfer of the 20 nm outer zones into a 75-nm-thick AZ resist.

C. Germanium and nickel patterning

Zone plates have been fabricated in both germanium and nickel, and both materials are good choices for high efficiency zone plates in the 2.4–4.5 nm wavelength range. The fabrication of nickel zone plates is more complicated: nickel

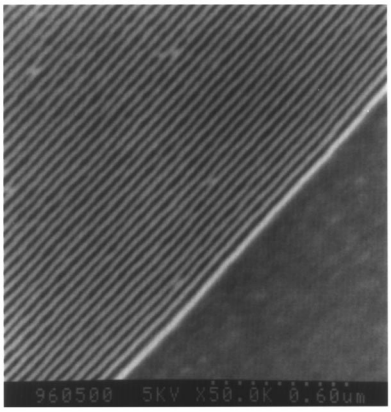

FIG. 2. SEM of the 20 nm outer zones after transfer into a 75-nm-thick layer of AZ resist.

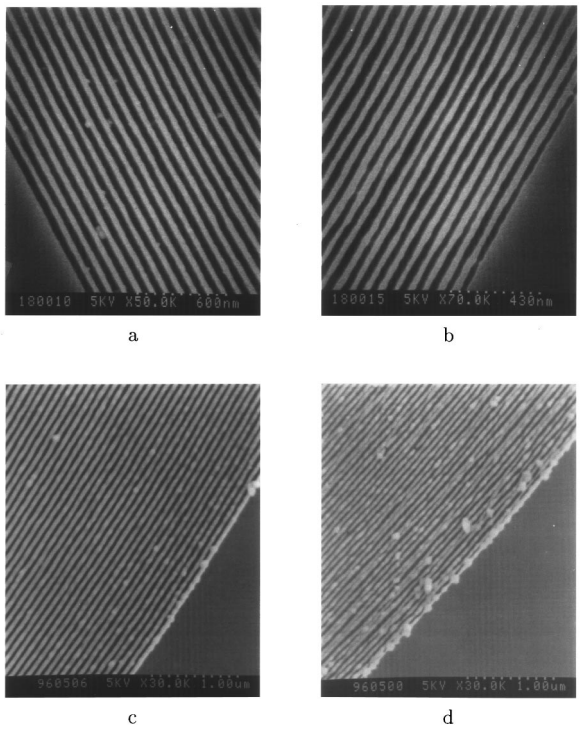

FIG. 3. SEMs of the outer zones of four zone plates: (a) Germanium zone plate with 40 nm outer zones, (b) 30 nm outer zones, (c) nickel zone plate with 40 nm outer zones, (d) 30 nm outer zones.

structures cannot be reactive ion etched and therefore must be electroplated. However, in the wavelength range of interest, nickel achieves the same efficiency as germanium with about half the thickness of material. A trilayer resist structure was used for the patterning of both materials.

The layers in the trilayer resist structure used for the patterning of the germanium features were, from bottom to top, 180 nm Ge, 85 nm AZ 4110, 10 nm Ge, and 30–40 nm PMMA.[13,14] We found it best to make all the layers in the trilayer resist structure as thin as possible, reducing the aspect ratios present during each step of the process. The Ge layers are formed by evaporation, and the resist layers by spinning. The AZ 4110 resist, purchased from Hoechst Celanese, is hard baked at 190 °C for 1 h. Reactive ion etching with selective gases is used to transfer the pattern through the layers into the germanium. CF_3Br (150 V, 10 mTorr) is used to etch the Ge layers, and O_2 (300 V, 10 mTorr) is used to etch the AZ layer and to clean the zone plate after the final Ge etch. It should be noted that CF_3Br is an ozone depleting gas, and it will be necessary to find a replacement gas. Figure 3 shows the outer zones of germanium zone plates with 30 and 40 nm outer zone widths. The germanium thickness of 180 nm has a theoretical diffraction efficiency of 10.4% at 3.2 nm.

For the patterning of nickel features, a trilayer resist is used in a method very similar to the germanium process. The thickness of the AZ photoresist (120 nm) needs to be slightly greater than the desired thickness of nickel (110 nm). The bottom layer of germanium is now replaced with a evaporated plating base of 5 nm of chrome and 10 nm of gold

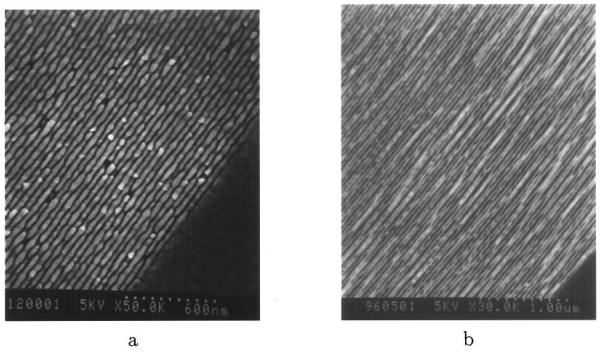

FIG. 4. SEMs showing the fabrication of 20 nm zone plates: (a) outer zones of 20 nm nickel zone plate, (b) outer zones of 20 nm germanium zone plate.

necessary for electrical conduction. Reactive ion etching steps are used as before to etch a pattern in the AZ resist. After the etching of the AZ resist a quick CF_3Br etch is used to remove the germanium masking layer. The AZ resist now serves as a form for the plating of nickel. The nickel plating is done in a sulphamate bath at ~35 °C with a plating current of 20 mA. Figure 3 shows the outer zones of nickel zone plates with 30 and 40 nm outer zone widths. The nickel thickness of 110 nm has a theoretical diffraction efficiency of 14.8% at 3.2 nm. The plating base of chrome and gold is left behind, and absorbs about 24% of the incident x rays. The diffraction efficiency does not account for this additional absorption. (It may be possible to remove the gold from the area in between the zones using argon ion milling.)

For comparison, zone plates with 20 nm outer zones were fabricated in both nickel and germanium. To make such fine structures, we chose to work with even thinner trilayer structures. The top resist was ~20 nm of calixarene instead of PMMA. Germanium zone plates, 100 nm thick, were fabricated using a 60-nm-thick AZ masking layer. Figure 4 shows that the germanium structures are not well formed. For the nickel zone plates, the AZ resist was 75 nm thick. Figure 4 shows the successful patterning of the outer zones of a 20 nm zone plate, before and after the nickel plating. Only 55 nm of nickel were plated, but the theoretical diffraction efficiency of 5.7% at a wavelength of 3.2 nm is more than sufficient for practical use.

D. Larger diameter zone plates

All the zone plates discussed so far have had a diameter of 80 μm. This diameter corresponds to the field size of the JEOL JBX-6000FS in a high resolution mode at 50 keV. Increasing the diameter of a zone plate increases the working distance of the zone plate, and for many applications a larger working distance than that provided by a 80-μm-diam zone plate is necessary. The fabrication of larger diameter zone plates can be achieved by stitching together multiple writing fields using the precise movement of the stage.

Zone plates 160 μm in diameter with 60 nm outer zone widths were fabricated by stitching four fields. (The zone plates have been used in the first Cryo-STXM experiments at X1A.)[15] Nine zone plates were fabricated, and the errors at

TABLE I. Measured diffraction efficiencies for several zone plates. These efficiencies are for zone plates 80 μm in diameter with central stops 35 μm in diameter. The largest zone widths in these zone plates are $\sim 2.3\delta_{rN}$, whereas unapodized zone plates have a largest zone width of more than 1 μm for parameters like those used here. The last column shows the measured efficiency minus the expected 24% reduction from the plating layer in the nickel zone plates.

Material (thickness) (nm)	Outer zone width, δ_{rN} (nm)	Wavelength (nm)	Measured efficiency (%)	Theoretical efficiency (%)	Subtract gold absorb.
Ge (180)	40	3.2	7.5	10.4	
Ge (180)	30	3.2	5.7	10.4	
Ge (180) (old software)	30	3.2	4.3	10.4	
Ni (110)	30	3.2	10.0	14.8	7.6%
Ni (55)	20	3.2	2.6	5.7	2.0%

the field boundaries varied from very slight to severe. Three zone plates had maximum stitching errors 15 nm or smaller, but a few had stitching errors as large as 60 nm. The source of the errors is still being investigated.

III. ANALYSIS

The zone plates have been tested in the STXM and their efficiencies have been measured. The diffraction efficiencies of some zone plates are shown in Table I. The 30 nm germanium zone plate fabricated after the software revision has a higher efficiency than the best 30 nm zone plate fabricated before the software revision. The 30 nm nickel zone plate has much higher diffraction efficiency than any 30 nm germanium zone plate, even after subtracting absorption from the plating base. The 2.0% efficiency of the 20 nm nickel zone plate is high enough efficiency for practical use in the STXM.

The diffraction efficiency of a region of a zone plate can be measured by using a pinhole aperture placed in the far field. The relationship between diffraction efficiency and zone width for three zone plates is shown in Fig. 5. This figure compares the diffraction efficiency of two 30 nm germanium zone plates (G-9 and J-9) and a 30 nm nickel zone plate (Q-7). For almost all zone plates that have been measured, the efficiencies become lower as the zone widths become finer. This drop in efficiency is partially due to the less perfect line shape and profiles of the outer zones. However the germanium zone plates show a greater drop in efficiency compared to the nickel zone plate. We believe this is in part due to incomplete etching of the Ge. [Note that scanning electron microscope (SEM inspection of the zones in Fig. 3 might predict that the germanium zone plates would be better.] The 30 nm zone plate fabricated after the software revision (J-4) has less of a drop in efficiency than the zone plate fabricated before the software revision (G-9). This may be due to the improved line shape control. A similar measurement showed that the diffraction efficiency of the 20 nm nickel zone plate was between 2.4% and 3.4% over all regions of the zone plate. This small variation in efficiency indicates that even the finest 20 nm outer zones are performing well.

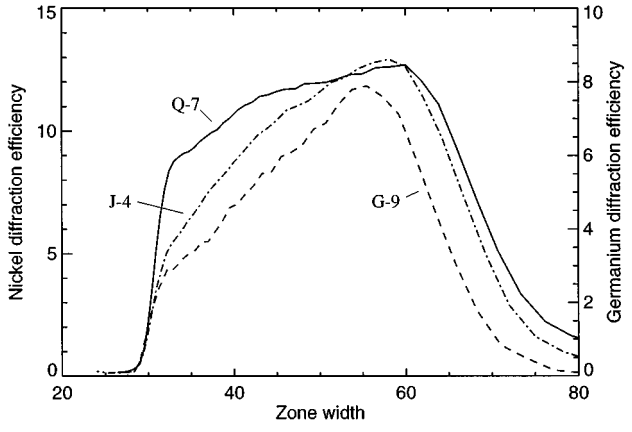

FIG. 5. Efficiencies for regions of three zone plates: (G-9) germanium zone plate fabricated before the software revision, (J-4) germanium zone plate fabricated after the software revision, and (Q-7) nickel zone plate. The nickel zone plate's efficiency is on a different scale than the two germanium zone plates.

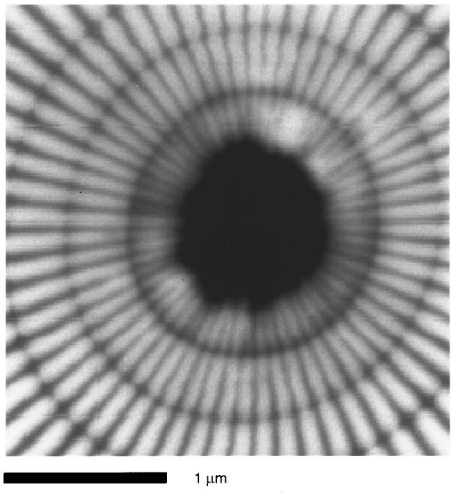

FIG. 6. STXM image of test pattern taken using a zone plate with 30 nm outer zones.

Figure 6 shows an image of a test pattern made using a 30 nm germanium zone plate in the STXM. At the inner ring of the test pattern features are 40 nm in size. Features <30 nm in size can be observed in this image. This is an improvement over the 45 nm zone plates which were the best we previously had available.[16]

IV. CONCLUSION

The process for fabricating zone plates has been optimized by improving the imaging resist, improving the pattern conversion, using a thin trilevel stack, and using electroplated layers of nickel. The nickel zone plates that have been fabricated are more efficient than comparable germanium zone plates despite a somewhat rougher appearance under SEM inspection. Zone plates with outer zone widths of 30 and 40 nm and high efficiencies can be fabricated using

PMMA. Zone plates with outer zone widths of 20 nm can be fabricated in thin nickel using calixarene resist. Thus, proliferation of zone plates with resolution in the 20 nm regime may now be possible with commercially available materials and nonspecialized *e*-beam exposure tools.

ACKNOWLEDGMENTS

The authors gratefully acknowledge J. Fujita and Y. Ohnishi for supplying the calixarene resist and the help of Ken Feder, Erik Anderson, Janos Kirz, Sue Wirick, and the Stony Brook group at the X1A beamline. The research was performed under partial support from the Electrical and Communications Systems division of the National Science Foundation under Grant No. ECS-9510499.

[1]X. Zhang, H. Ade, C. Jacobsen, J. Kirz, S. Lindaas, S. Williams, and S. Wirick, Nucl. Instrum. Methods Phys. Res. A **347**, 431 (1994).
[2]A. P. Smith, J. H. Laurer, H. W. Ade, S. D. Smith, A. Ashraf, and R. J. Spontak, Macromolecules **30**, 663 (1997).
[3]M. J. Simpson and A. G. Michette, Opt. Acta **30**, 1455 (1983) (now Journal of Modern Optics).
[4]C. David, B. Kaulich, R. Medenwaldt, M. Hettwer, N. Fay, M. Diehl, J. Thieme, and G. Schmahl, J. Vac. Sci. Technol. B **13**, 2762 (1995).
[5]E. H. Anderson, V. Boegli, and L. P. Muray, J. Vac. Sci. Technol. B **13**, 2525 (1995).
[6]P. Charalambous, P. Anastasi, R. E. Burge, and K. Popova, in *X-ray Microbeam Technology and Applications*, edited by W. Yun (Society of Photo-Optical Instrumentation Engineers, Bellingham, WA, 1995), Vol. 2516, pp. 2–14.
[7]J. Pawlak, P. C. Cheng, and D. M. Shinozaki, in *X-ray Microscopy: Instrumentation and Biological Applications*, edited by P. C. Cheng and G. J. Jan (Springer, Berlin, 1987).
[8]R. E. Howard, E. L. Hu, L. D. Jackel, P. Grabby, and D. M. Tennant, Appl. Phys. Lett. **36**, 596 (1980).
[9]S. J. Spector, Ph.D. thesis, Department of Physics, State University of New York at Stony Brook, 1997.
[10]A. Ozawa, T. Tamamura, T. Ishii, H. Yoshihara, and T. Kagoshima, Microelectron. Eng. **35**, 525 (1997).
[11]X. Zhang, C. Jacobsen, S. Lindaas, and S. Williams, J. Vac. Sci. Technol. B **13**, 1477 (1995).
[12]J. Fujita, Y. Ohnishi, Y. Ochiai, and S. Matsui, Appl. Phys. Lett. **68**, 1297 (1996).
[13]D. M. Tennant, E. L. Raab, M. M. Becker, M. L. O'Malley, J. E. Bjorkholm, and R. W. Epworth, J. Vac. Sci. Technol. B **8**, 1970 (1990).
[14]S. J. Spector, C. J. Jacobsen, and D. M. Tennant, in *X-Ray Microscopy and Spectromicroscopy*, Springer Series in Optical Sciences, edited by J. Thieme, G. Schmahl, E. Umbach, and D. Rudolph (Springer, Berlin, 1997).
[15]J. Maser, C. Jacobsen, A. Osanna, S. Wang, A. Kalinovsky, J. Kirz, S. Spector, and J. Warnking, in *X-Ray Microscopy and Spectromicroscopy*, Springer Series in Optical Sciences, edited by J. Thieme, G. Schmahl, E. Umbach, and D. Rudolph (Springer, Berlin, 1997).
[16]C. Jacobsen, S. Williams, E. Anderson, M. T. Browne, C. J. Buckley, D. Kern, M. Rivers, and X. Zhang, Opt. Commun. **86**, 351 (1991).